Supporting Information

Dual Switchable Molecular Tweezers Incorporating Anisotropic Mn^{III}-Salphen Complexes

Benjamin Doistau,[†a] Lorien Benda,[†a] Jean-Louis Cantin,[b] Olivier Cador,[c] Fabrice Pointillart,[c] Wolfgang Wernsdorfer,[d] Lise-Marie Chamoreau,[a] Valérie Marvaud,[a] Bernold Hasenknopf[a] and Guillaume Vives*[a]

Table of contents

Mass spectra

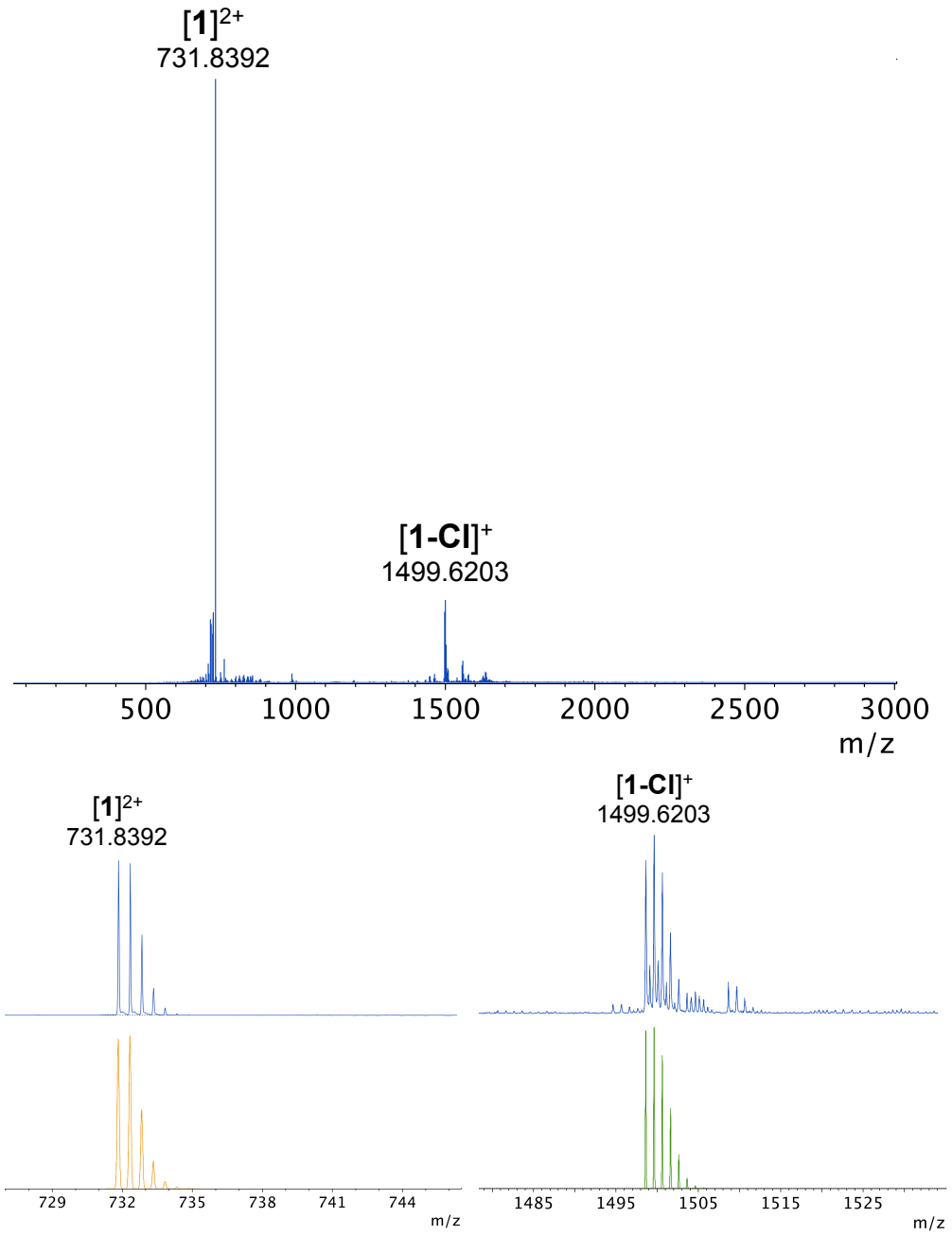

Figure S1. ESI-TOF HRMS spectra of tweezers **1-Cl$_2$**. Full spectrum and zoom with isotopic pattern experimental (top) and calculated (bottom).

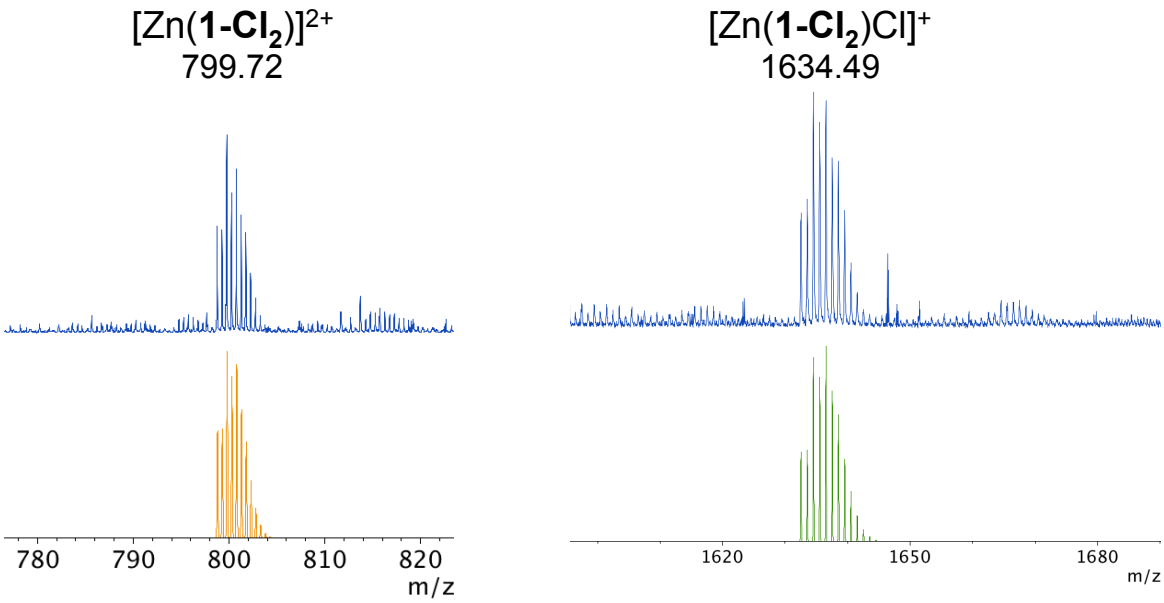

Figure S2. ESI-TOF MS spectra of closed tweezers [Zn(**1-Cl₂**)]Cl_2 and isotopic pattern experimental (top) and calculated (bottom).

Zn-closed UV-Vis titrations and XRD

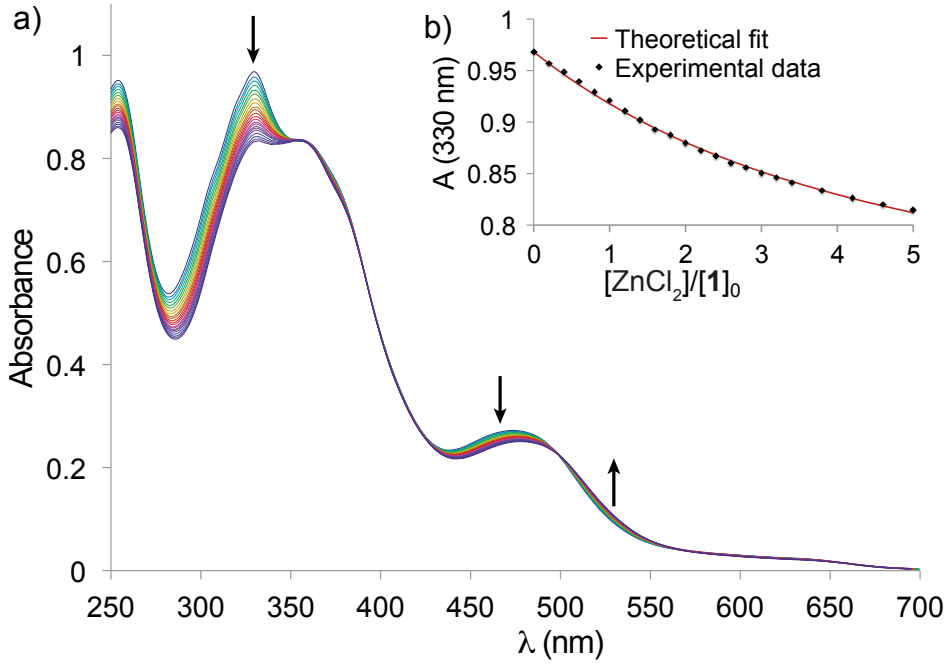

Figure S3. a) UV-Vis titration of **1-Cl$_2$** (1.0×10^{-5} mol·L^{-1}) by $ZnCl_2$ in MeOH. b) Absorption at 330 nm and fitting with a 1:1 binding model.

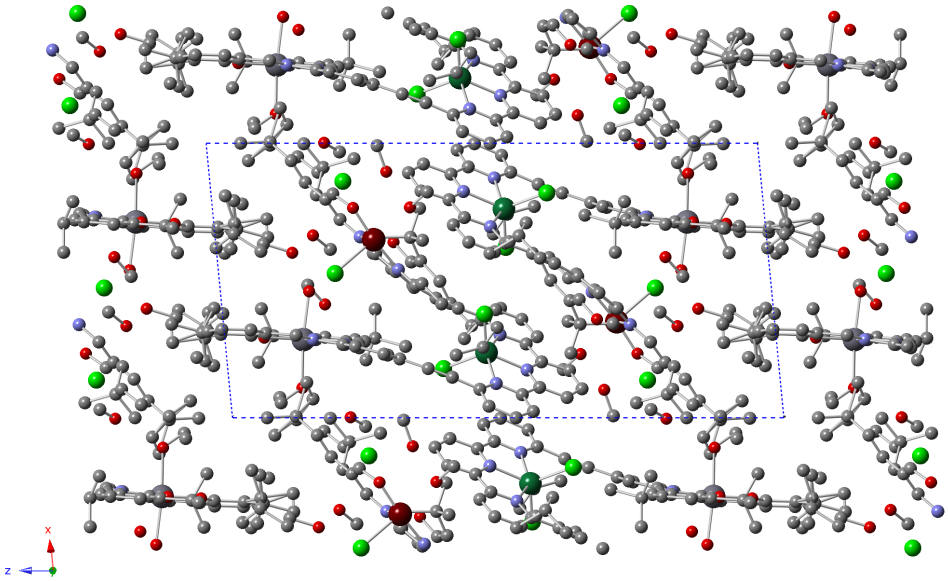

Figure S4. Packing of closed tweezers along crystallographic axis b.

Cyanide binding: UV-Vis titrations and EPR spectra

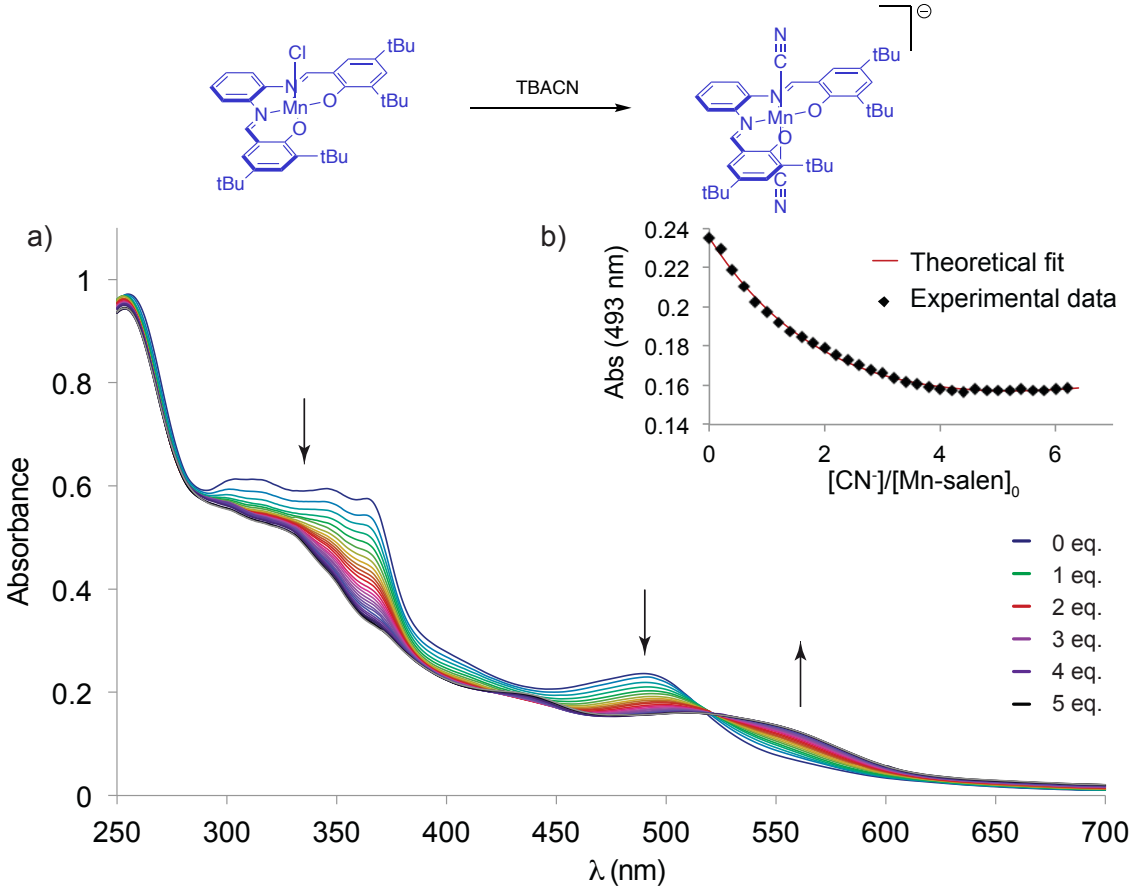

Figure S5. a) UV-Vis titration of [Mn-salphenCl] (3.0×10^{-5} mol·L^{-1}) by TBACN in $CHCl_3$. b) Absorption at 493 nm and fitting with a 1:2 binding model.

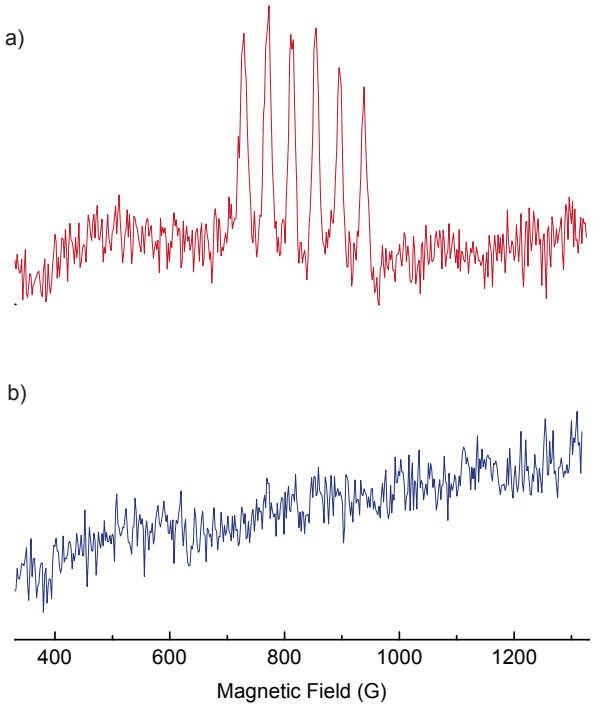

Figure S6. X-band EPR spectra of a) [Mn-salphenCl] and b) $[Mn\text{-salphen}(CN)_2]^-$ (in MeOH at 5K) in parallel mode.

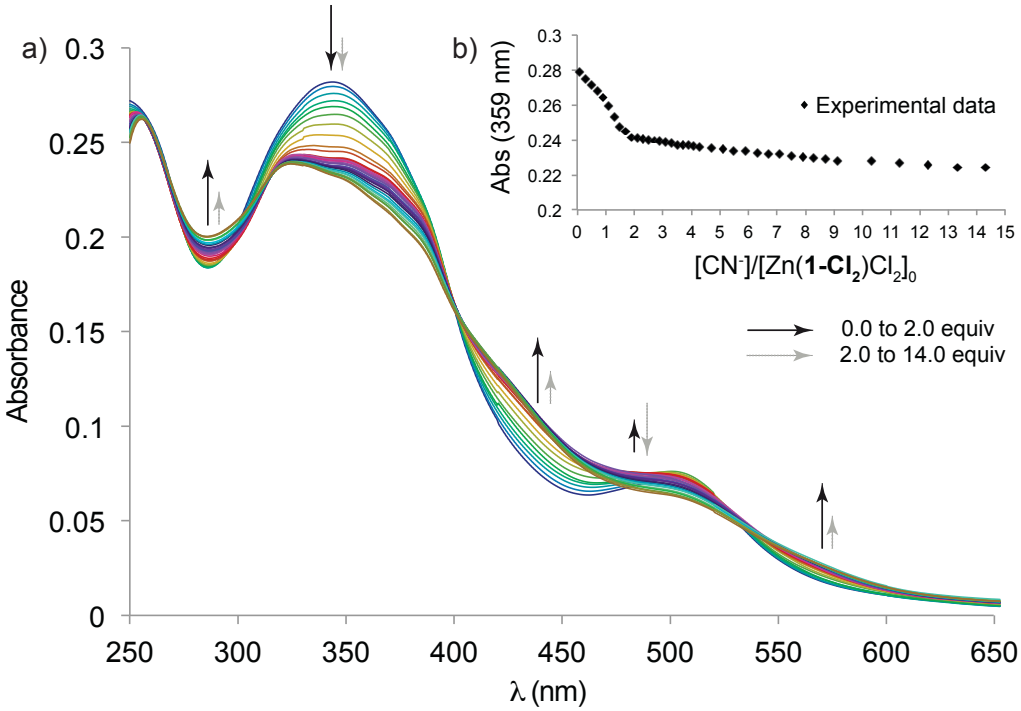

Figure S7. UV-Vis titration of [Zn(**1-Cl₂**)Cl_2] (5.0×10^{-6} mol·L^{-1}) by TBACN in $CHCl_3$.

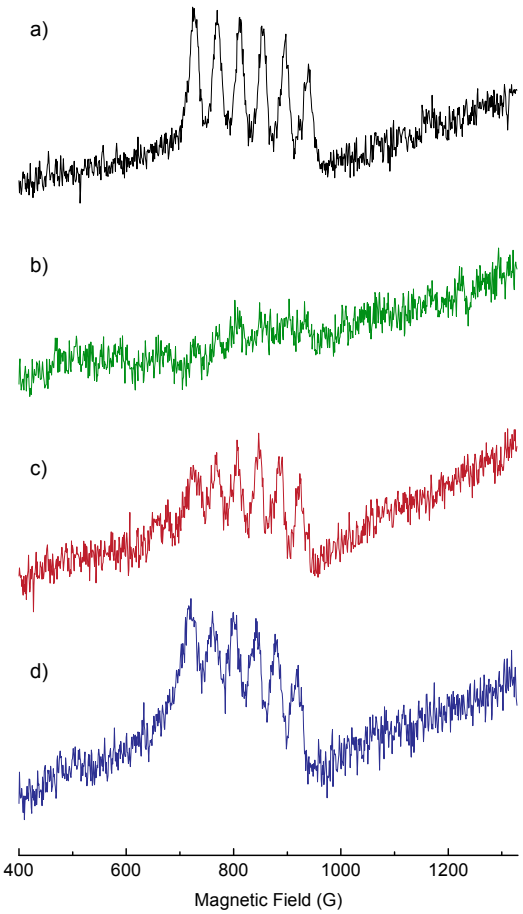

Figure S8. X-band EPR spectra of a) tweezers **1-Cl₂**; b) [Zn(**1-Cl₂**)Cl_2] + CN^-; c) [Zn(**1-Cl₂**)Cl_2] + excess CN^-; d) tweezers **1-Cl₂** + CN in parallel mode (1.0×10^{-4} mol·L^{-1} in MeOH at 5K).

SQUID Magnetometry

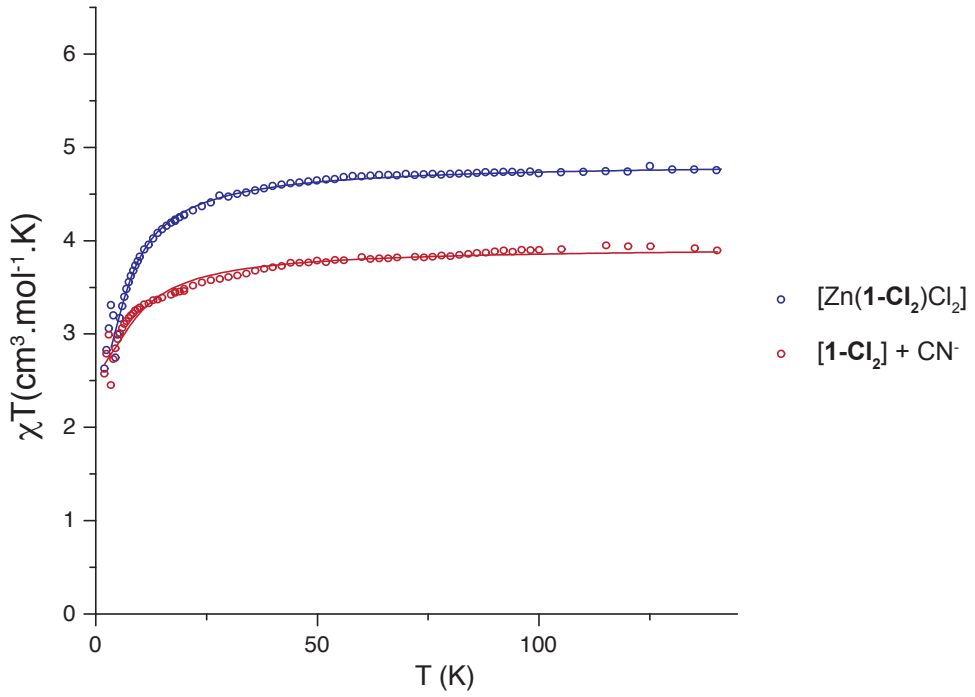

Figure S9. $\chi T = f(T)$ of closed tweezers [Zn(**1-Cl₂**)Cl_2] (blue), and [**1-Cl₂**] with CN^- (red), in frozen $CHCl_3$ solution.

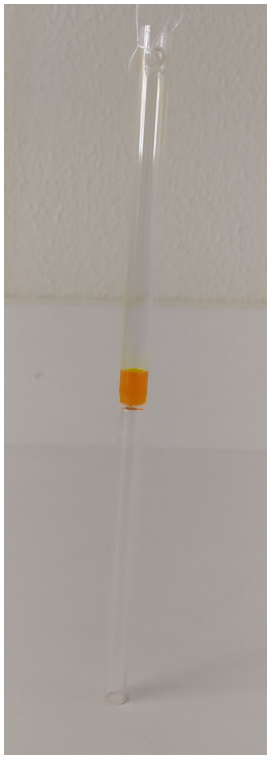

Figure S10. Picture of the closed quartz tube sample holder with an illustrative sample solution used for SQUID magnetometry experiments.

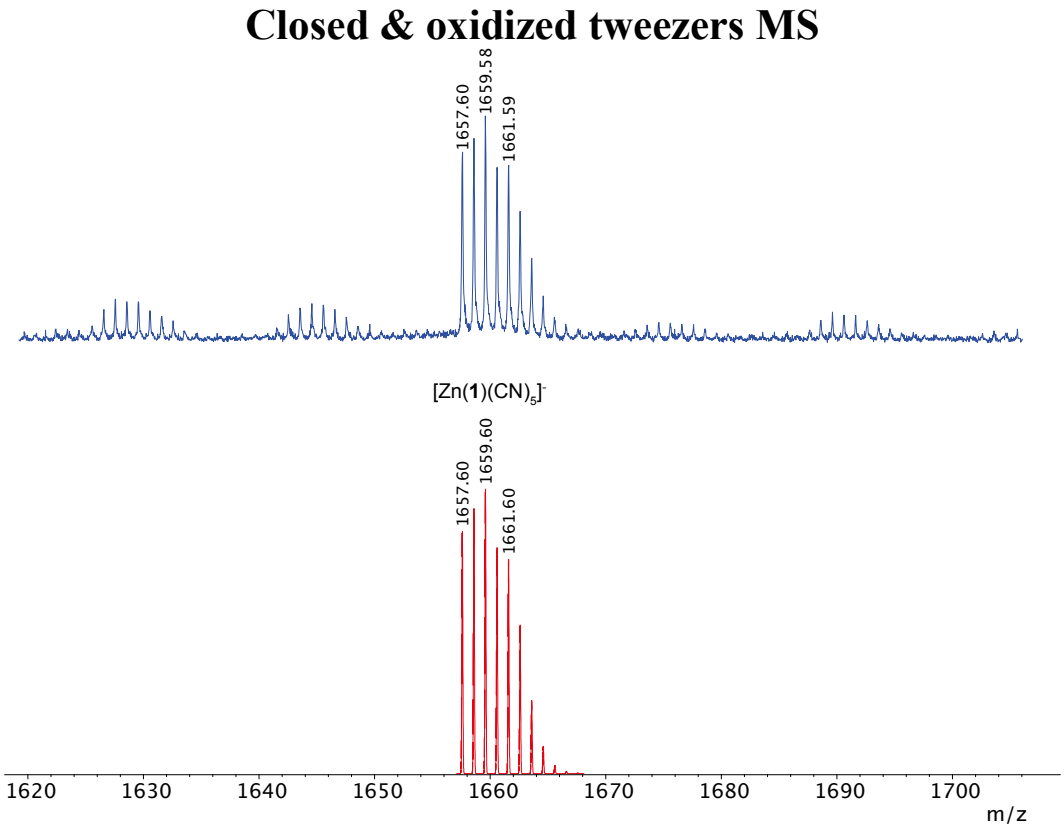

Figure S11. ESI-TOF MS spectrum of $[Zn(\mathbf{1})(CN)_5]^-$ and isotopic pattern experimental (top) and calculated (bottom).

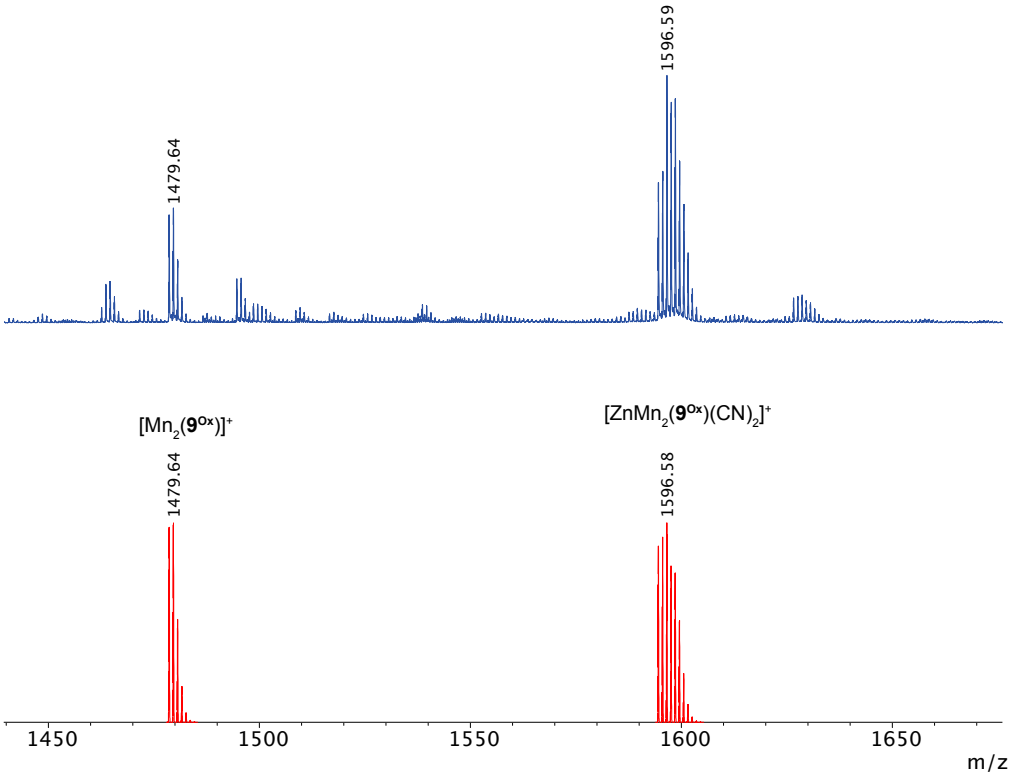

Figure S12. ESI-TOF MS spectrum of oxidized tweezers $[Mn^{III}_2(\mathbf{9^{Ox}})]$ isotopic pattern experimental (top) and calculated (bottom).

NMR spectra of compounds

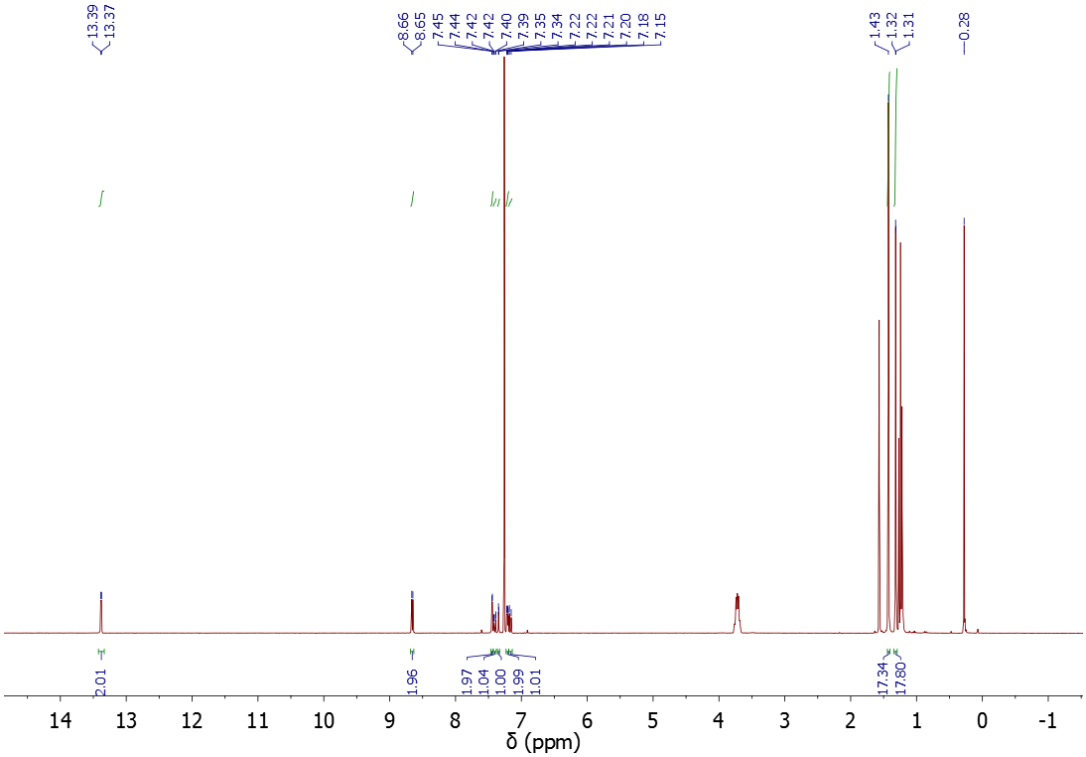

Figure S13. ^{1}H NMR (400 MHz, 300 K) spectrum of **6** in $CDCl_3$.

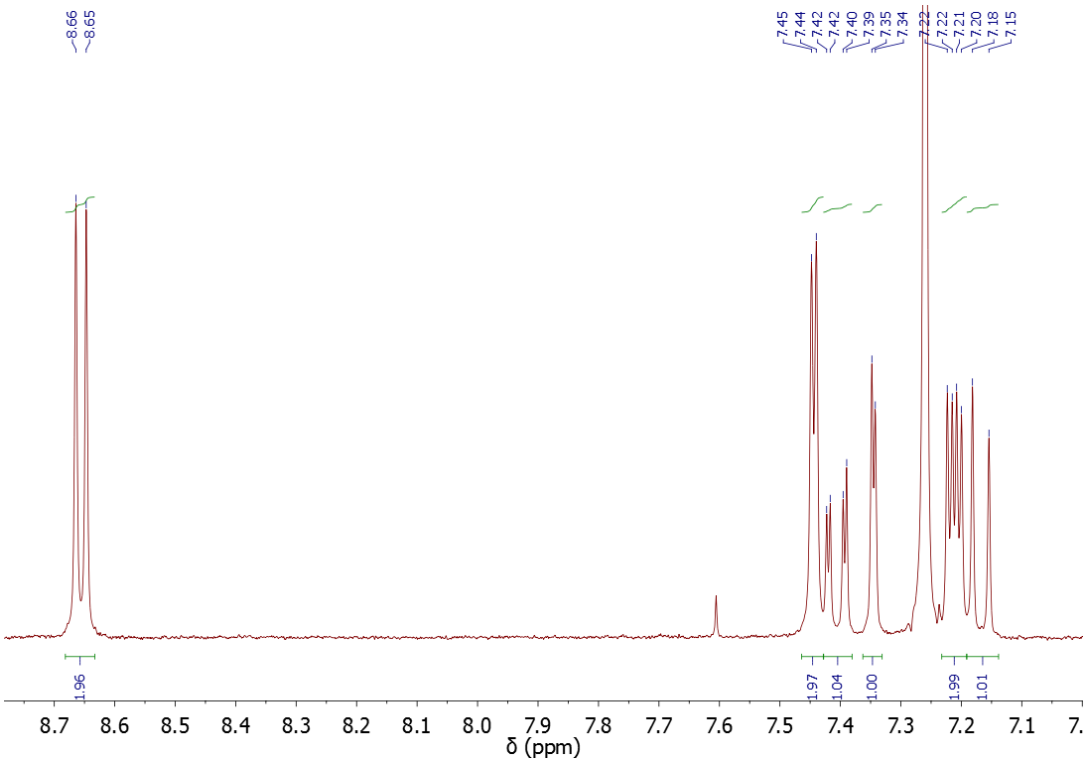

Figure S14. Aromatic region of ^{1}H NMR (400 MHz, 300 K) spectrum of **6** in $CDCl_3$

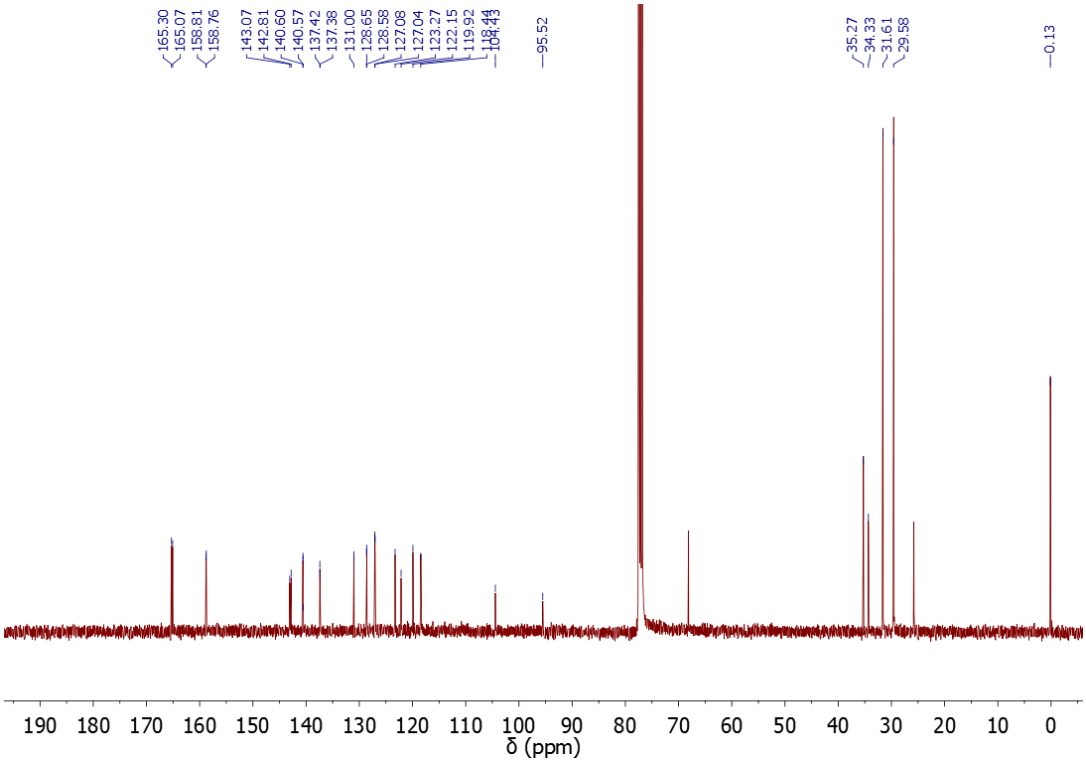

Figure S15. ^{13}C NMR (100 MHz, 300 K) spectrum of **6** in $CDCl_3$.

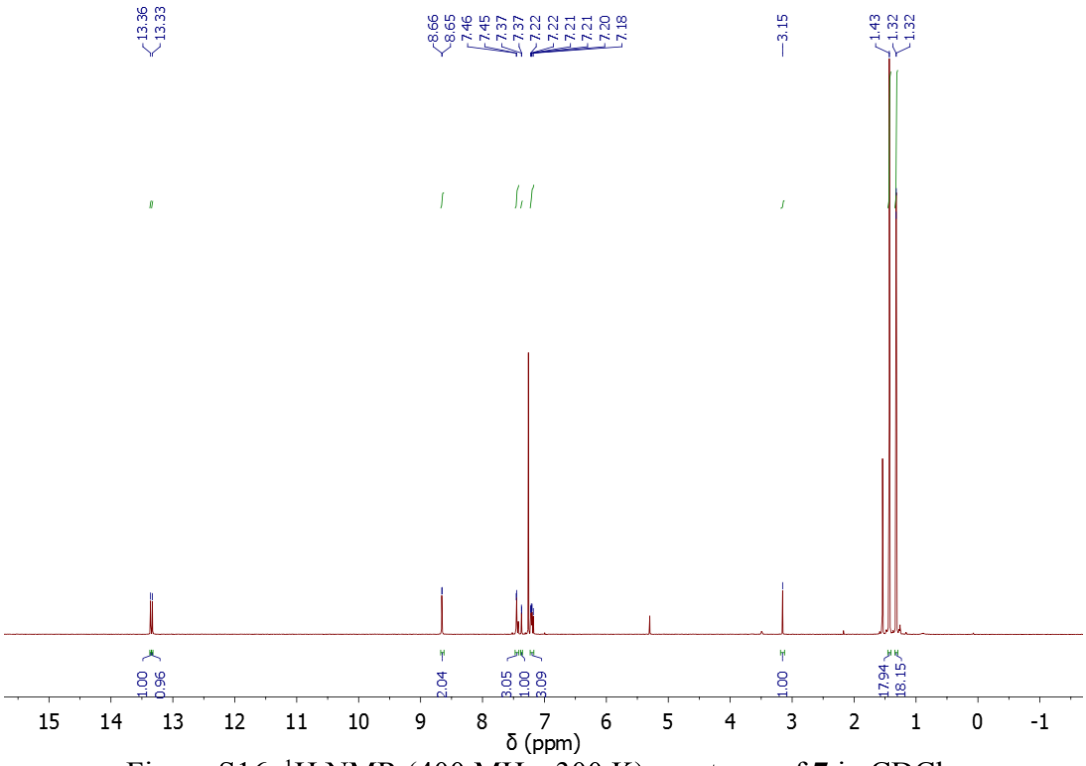

Figure S16. ^{1}H NMR (400 MHz, 300 K) spectrum of **7** in $CDCl_3$.

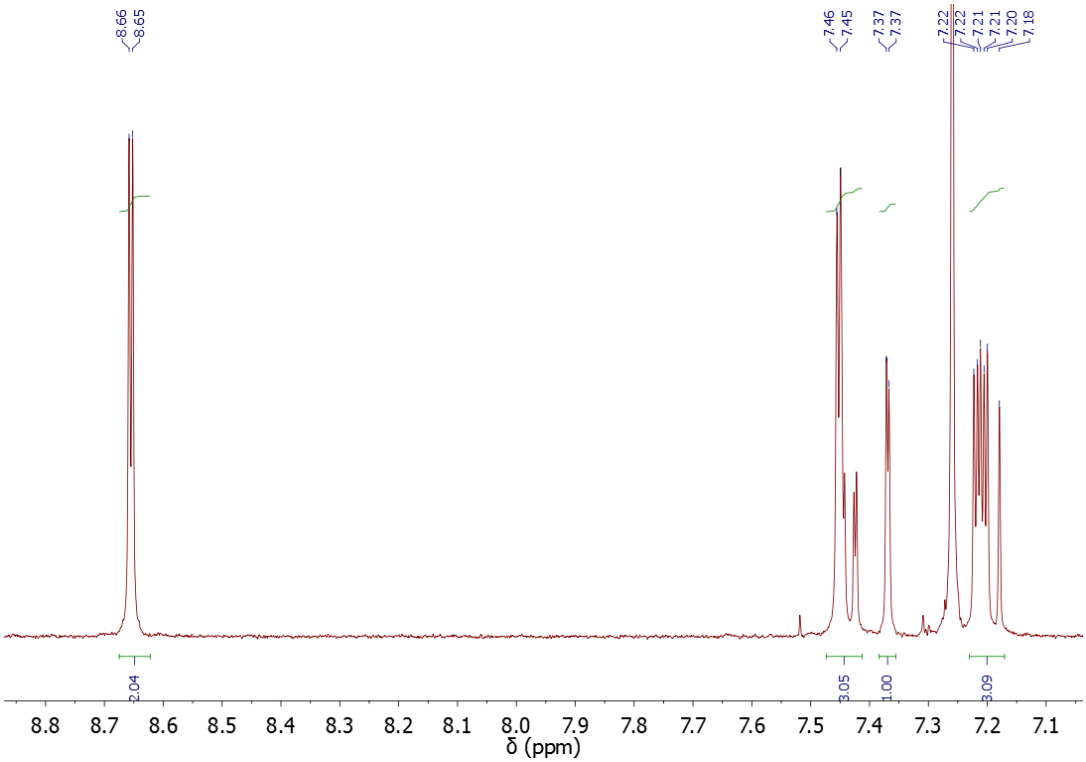

Figure S17. Aromatic region of ^{1}H NMR (400 MHz, 300 K) spectrum of **7** in $CDCl_3$

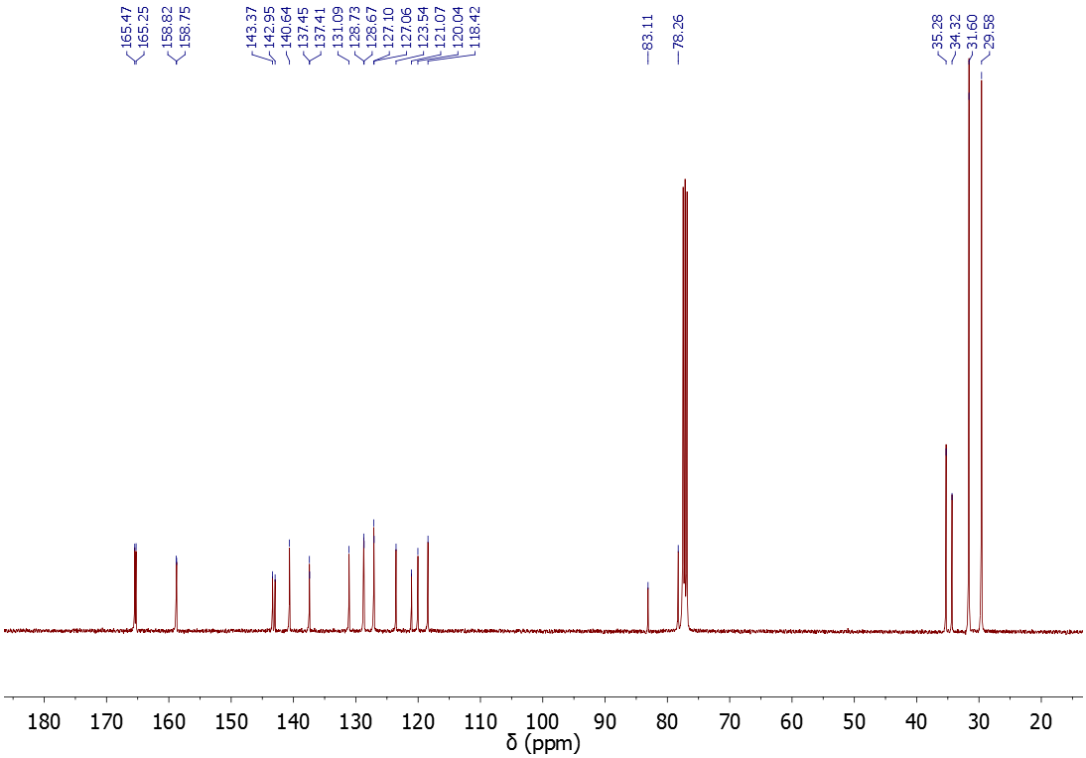

Figure S18. ^{13}C NMR (100 MHz, 300 K) spectrum of **7** in $CDCl_3$.

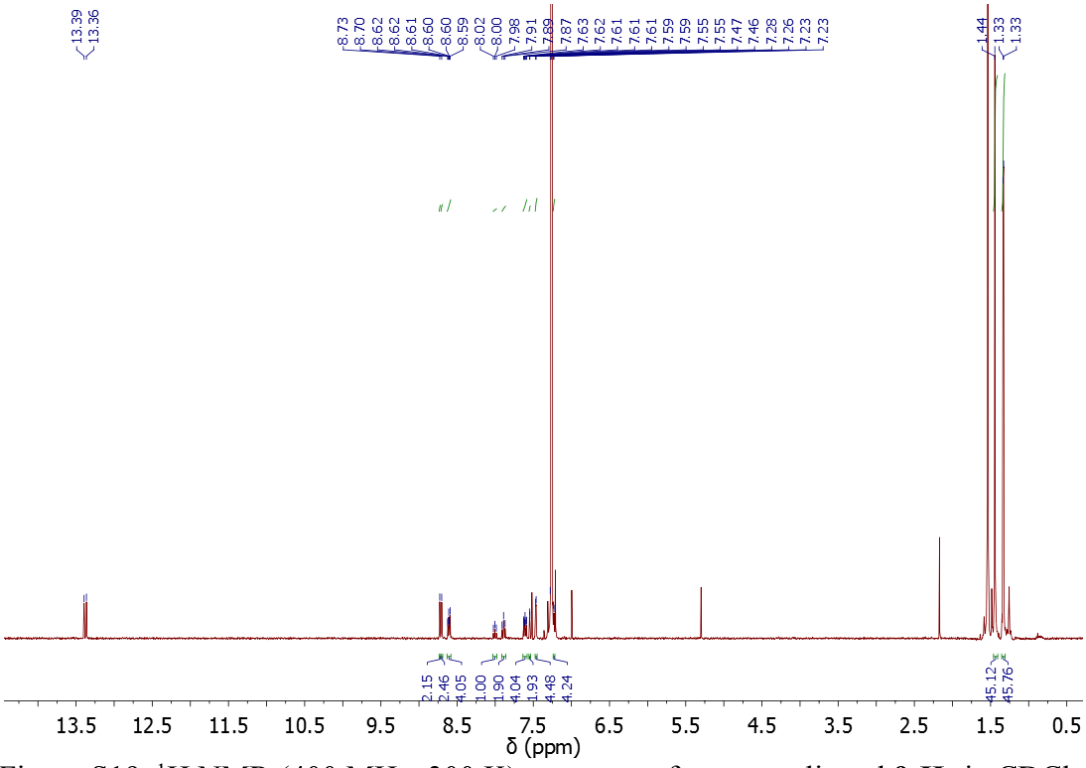

Figure S19. ^{1}H NMR (400 MHz, 300 K) spectrum of tweezers ligand **9-H$_4$** in $CDCl_3$.

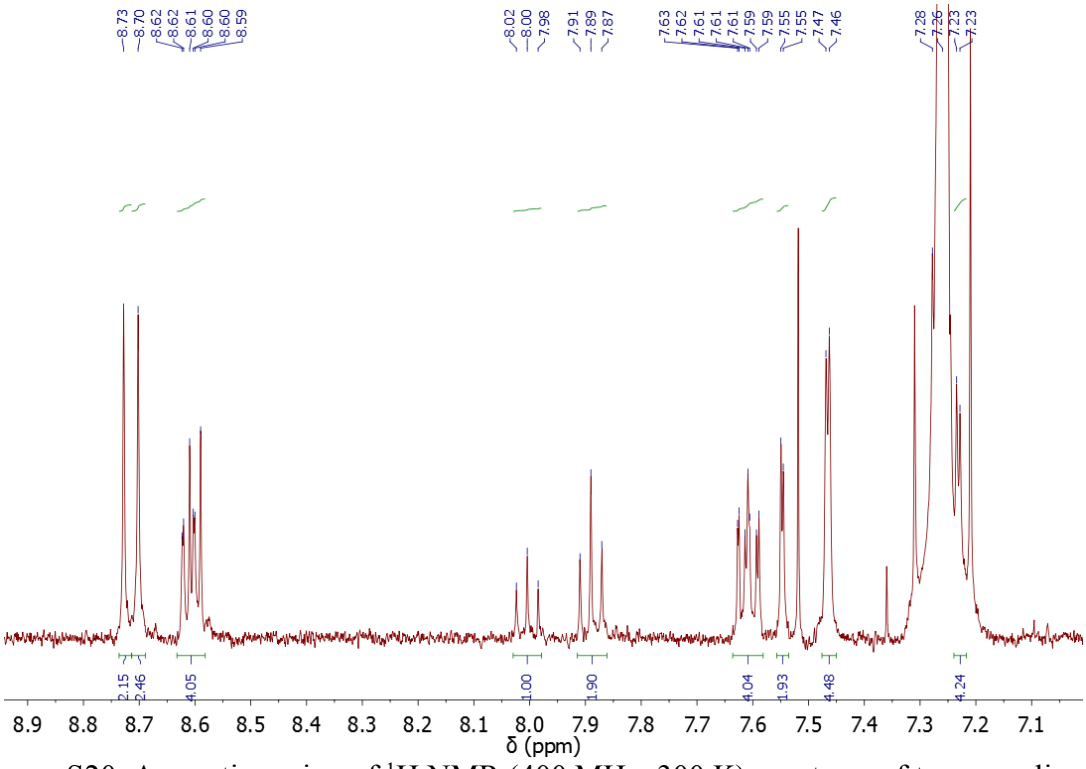

Figure S20. Aromatic region of ^{1}H NMR (400 MHz, 300 K) spectrum of tweezers ligand **9-H$_4$** in $CDCl_3$

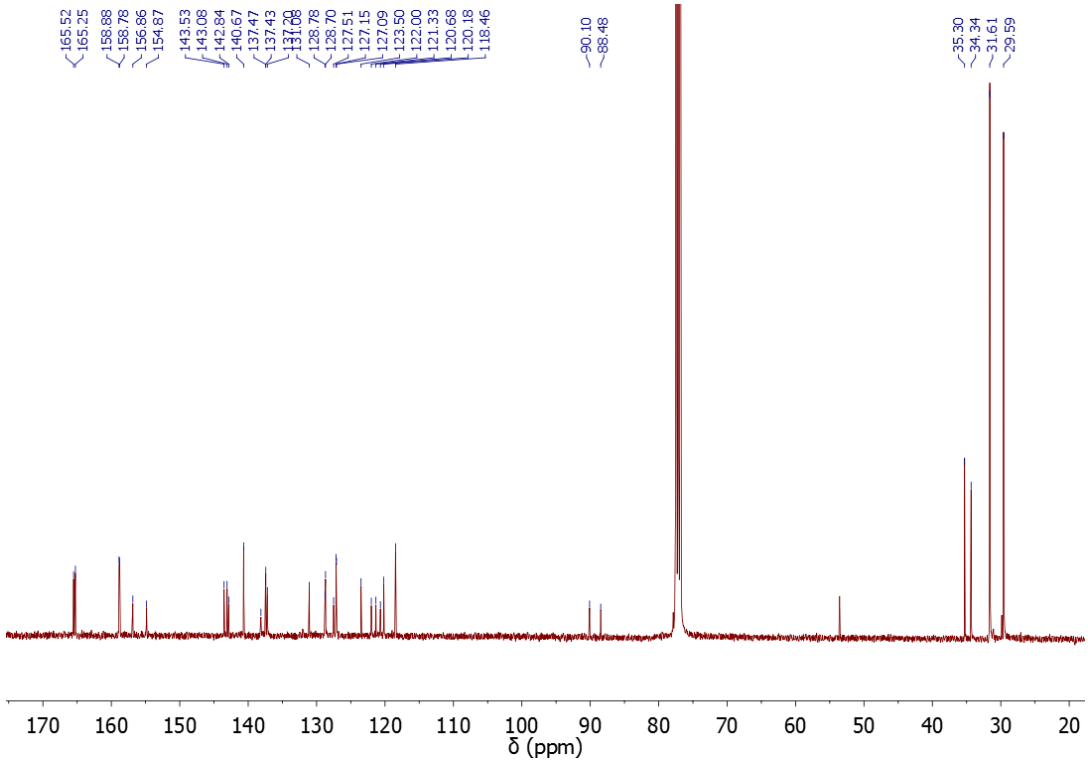

Figure S21. ^{13}C NMR (100 MHz, 300 K) spectrum of tweezers ligand **9-H$_4$** in $CDCl_3$.

IR spectra of compounds

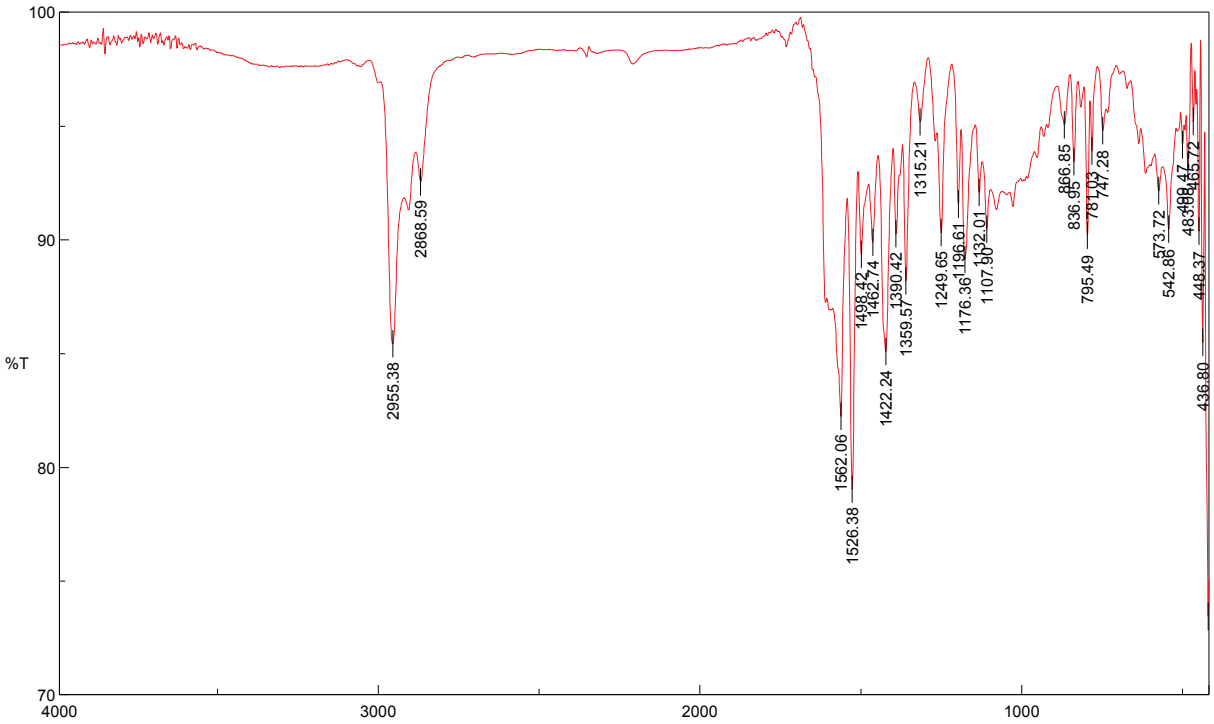

Figure S22. FTIR spectrum of open tweezers **1-Cl$_2$**.

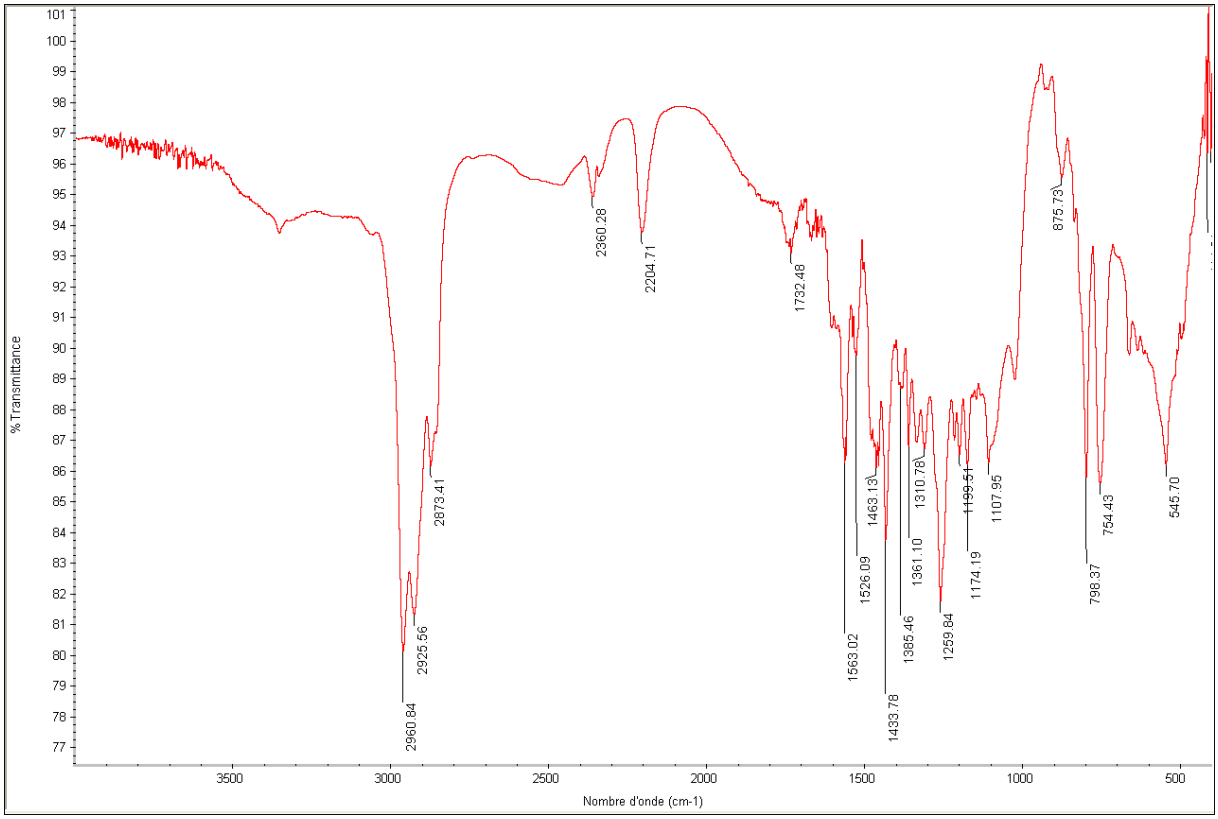

Figure S23. FTIR spectrum of CN-closed tweezers

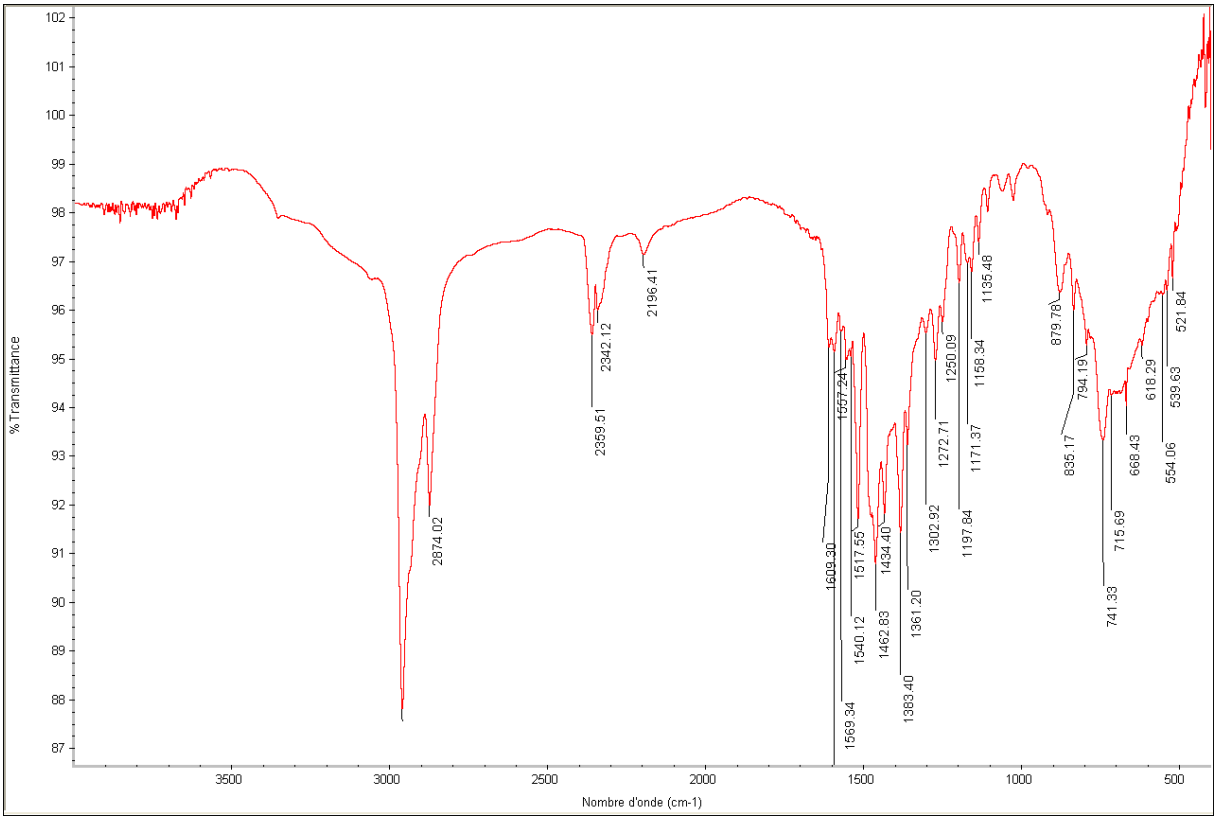

Figure S24. FTIR spectrum of $[Mn\text{-}salphen(CN)_2]^-$